Increasing the molecular weight of conjugated polyelectrolytes improves the electrochemical stability of their pseudocapacitor gels

Vázquez, Ricardo Javier; Quek, Glenn; McCuskey, Samantha R.; Llanes, Luana; Kundukad, Binu; Wang, Xuehang; Bazan, Guillermo C.

DOI
10.1039/d2ta05053f

Publication date
2022

Document Version
Final published version

Published in
Journal of Materials Chemistry A

Citation (APA)
Vázquez, R. J., Quek, G., McCuskey, S. R., Llanes, L., Kundukad, B., Wang, X., & Bazan, G. C. (2022). Increasing the molecular weight of conjugated polyelectrolytes improves the electrochemical stability of their pseudocapacitor gels. *Journal of Materials Chemistry A*, *10*(40), 21642-21649. https://doi.org/10.1039/d2ta05053f

Journal of Materials Chemistry A

ROYAL SOCIETY OF CHEMISTRY

PAPER

View Article Online
View Journal | View Issue

Cite this: J. Mater. Chem. A, 2022, 10, 21642

Increasing the molecular weight of conjugated polyelectrolytes improves the electrochemical stability of their pseudocapacitor gels†

Ricardo Javier Vázquez, ‡[abc] Glenn Quek,‡[a] Samantha R. McCuskey,[ac] Luana Llanes,[d] Binu Kundukad,[c] Xuehang Wang[e] and Guillermo C. Bazan *[abc]

Received 25th June 2022
Accepted 20th September 2022

DOI: 10.1039/d2ta05053f

rsc.li/materials-a

Conjugated polyelectrolyte (CPE) hydrogels synergize the electrical properties of redox-active polymers with the physical properties of hydrogels. Of particular relevance is their implementation as pseudocapacitors due to their high ionic conductivity, strong ionic–electronic coupling, and large electroactive surface area. To date, efforts to improve the cycling stability of such hydrogels are predominated by the use of additives – optimization of the CPE's intrinsic properties remains underexplored. Herein, the systematic increase in the molecular weight (MW) of a self-doped CPE, namely CPE-K, has been demonstrated as an effective strategy to enhance the cycling stability of the resulting hydrogel. At high MW, mechanically stronger hydrogels were obtained with a specific capacitance as high as 88 ± 4 F g^{-1} at 0.25 A g^{-1} and a cycling stability of 76% capacitance retention after 100 000 cycles at 2.5 A g^{-1}. Furthermore, this strategy yields a wider working pseudocapacitive window, less internal resistance, and higher ionic conductivity within the 3D conductive network. We attribute the enhanced electrochemical performance to stronger inter-chain contacts for optimal morphological organization, as revealed by rheological measurements, resulting in stress-tolerant hydrogels with a higher degree of percolation within a 3D conductive network. These results position CPE-K hydrogels as a state-of-the-art organic material for long-term pseudocapacitive technologies and potentially for the next generation of multi-functional pseudocapacitive devices that go beyond high energy density and power density.

1 Introduction

Pseudocapacitors display intermediate properties between rechargeable batteries and capacitors, occupying a niche position with respect to delivering their power and energy density.[1–3] Their electrical energy storing mechanism relies on fast and reversible faradaic redox reactions at electrode interfaces or pseudocapacitive ion intercalation, which differs from the purely electrostatic nature of electric double-layer capacitors.[4] Organic semiconductors are relevant in this respect since they may provide cost-effective alternatives to the predominantly used rare transition metal oxide-based electroactive materials.[5] Indeed, one finds substantial interest in using conjugated polymers for developing lightweight, affordable, and high-performance pseudocapacitors.[6]

Improving the cycling stability of conjugated polymer (CP) pseudocapacitors remains an area of opportunity.[1,7] Challenges arise due to volumetric changes over repeated charge/discharge cycles.[8] For instance, polypyrrole (PPy) and polyaniline (PAni) possess specific capacitance values of 620 F g^{-1} and 750 F g^{-1}, respectively, but their performance decreases more than 50% from their initial values after 4000 charge/discharge cycles.[7,8] Another example is poly(3,4-ethylenedioxythiophene):poly(styrene sulfonate) (PEDOT:PSS), for which a specific capacitance value of 210 F g^{-1} has been reported. However, the initial value decreases to 80% within the first 1200 charge/discharge cycles.[9] Nanostructuring by employing electro-polymerization or mixing carbonaceous materials into the polymeric structure, such as graphene derivatives or polysulfonated aromatics, has circumvented poor cycling stability.[8,10,11] Adding such carbonaceous materials helps in creating non-covalent rigidifying bridges between polymer chains and also in opening channels within the structure to facilitate ion transport.[8,12]

[a]Departments of Chemistry and Chemical & Biomolecular Engineering, National University of Singapore, Singapore 119077. E-mail: chmbgc@nus.edu.sg

[b]Institute for Functional Intelligent Materials, National University of Singapore, 117544, Singapore

[c]Singapore Centre for Environmental Life Sciences Engineering, Nanyang Technological University, Singapore 639798

[d]Department of Chemistry and Biochemistry, University of California, Santa Barbara, CA, USA

[e]Department of Radiation Science and Technology, Delft University of Technology, Delft 2629 JB, The Netherlands

† Electronic supplementary information (ESI) available. See https://doi.org/10.1039/d2ta05053f

‡ These authors contributed equally to this work.

Conjugated polyelectrolytes (CPEs) contain conjugated backbones that possess pendant side chains with ionic functionalities, granting them unique advantages over conventional CPs.[11,13] Of particular relevance is their implementation as pseudocapacitive hydrogels owing to their excellent ion conductivities, high degree of ionic–electronic coupling, water processability, self-doping properties, and large electrode/electrolyte interfacial areas.[11,14–17] Furthermore, their excellent shape adaptability and softness present them as attractive materials for flexible devices with sustained capacitive performance when bent or stretched.[18] Lastly, hydrogels can be designed to interface with living systems. This particular feature unlocks a niche dual-mode function within the CPE hydrogels, making them capable of switching between biocurrent generation and electrochemical energy storage by utilizing an external stimulus, namely the addition or removal of Mg^{2+}.[19,20] Consequently, these properties open up opportunities for devising the next generation of multi-functional pseudocapacitive devices that go beyond high energy density and power density.[11]

Poly[2,6-(4,4-bis-potassium butanylsulfonate-4*H*-cyclopenta-[2,1-*b*;3,4-*b*′]-dithiophene)-*alt*-4,7-(2,1,3-benzothiadiazole)] (CPE-K, see Fig. 1) is a self p-doped CPE that forms a hydrogel through self-assembly *via* electrostatic and hydrophobic interactions once a critical concentration is reached.[14,17,19–21] CPE-K hydrogels have reported specific capacitance values of up to 75 F g^{-1}, albeit with low cycling stabilities of 40% capacitance retention after 1000 charge/discharge cycles.[15,19,20] Previous efforts to improve the cycling stability involve the incorporation of electrostatic interchain crosslinkers, such as multi-cationic 2D electrolytes and Mg^{2+} ions. The resulting mechanically rigidified CPE-K hydrogels exhibit increased capacitance retention of ~80% after 1000 charge/discharge cycles.[14,21] Although these stabilities are similar to other CP systems, further improvements should be attainable given that the dynamic nature of hydrogels can accommodate volumetric changes that occur over repeated charge/discharge cycles without adverse structural degradations.[7,8,11,14,21]

In this contribution, we sought a new strategy to improve the pseudocapacitive cycling stability of CPE-based hydrogels beyond using conventional additives. We hypothesized that increasing the molecular weight (MW) of the CPE chains will improve interchain packing in the self-assembled hydrogel to form a more percolated network with higher conductivities and greater mechanical strength. To this end, a high MW CPE-K sample was obtained by fine-tuning the monomer ratios in the Suzuki polycondensation. We show that the specific capacitance of the resulting high MW CPE-K hydrogel is 88 ± 4 F g^{-1} with a significantly improved cycling stability over previous reports – 76% capacitance retention after 100 000 charge/discharge cycles. This high cycling stability demonstrates the potential of such self-doped high MW CPE hydrogels for high-performance electrochemical energy storage and conversion applications.[22,23]

2 Results and discussion

Following Carothers equation for condensation polymerization reactions, an equimolar ratio of bifunctional reactive monomers should lead to a polymer with the highest MW.[24] This ideal ratio is difficult to achieve in practice due to the presence of impurities and undesirable side reactions, such as deborylation in Suzuki cross-coupling polymerizations.[25] We thus examined the effect of minor deviations from an apparent 1 : 1 stoichiometry, as shown in Fig. 2 and Scheme S1.† These studies revealed that adding 1.1 equivalents of 2,1,3-benzothiadiazole-4,7-bis(boronic acid pinacol ester) (BT), as determined by the weight of the reactants used, relative to potassium 4,4′-(2,6-dibromo-4*H*-cyclopenta[2,1-*b*:3,4-*b*′]dithiophene-4,4-diyl) bis(butane-1-sulfonate) ($CPDT(SO_3K)_2Br_2$), yields a high MW CPE-K with a M_n of 31 960 g mol^{-1}. A 1 : 1 stoichiometry yielded a medium MW CPE-K with a number average molecular weight (M_n) of 23 038 g mol^{-1}. Using a 1 : 0.9 stoichiometry yielded a low MW CPE-K with a number average molecular weight (M_n) of 18 794 g mol^{-1}, see Fig. S1† for GPC analysis. No differences across the polymers were observed when measuring their ^{1}H-NMR spectra, cyclic voltammetry response as thin films, or optical absorption profiles (see Fig. S2, S3 and S4,† respectively). Scanning electrode microscopy (SEM) was carried out to evaluate the microscopic topography and nanoscopic landscape of the CPE-K hydrogels with varying MW, see Fig. S5.† However, no evident differences in topography or morphology were observed for the investigated systems under the tested conditions. Therefore, we proceeded to characterize the influence of MW on the pseudocapacitive properties of CPE-K in its hydrogel form (20 mg CPE-K in 1 mL of Milli-Q water. See Fig. S6† for reactor details).[20]

CPE-K hydrogels were first probed by cyclic voltammetry (CV) to investigate the influence of MW on their electrochemical properties. CV traces were measured daily at a rate of 5 mV s^{-1} until the hydrogels stabilized through ion exchange with the

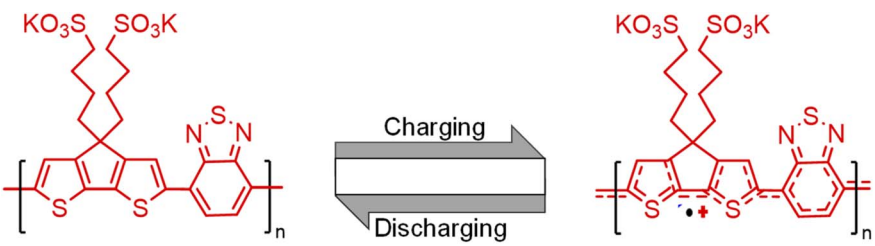

Fig. 1 Mechanism of charging/discharging in self-doped p-type CPE-K. Left: undoped (neutral) conjugated polymer. Right: doped (oxidized) CPE-K with stored positive charges compensated by anions from the electrolyte solution.

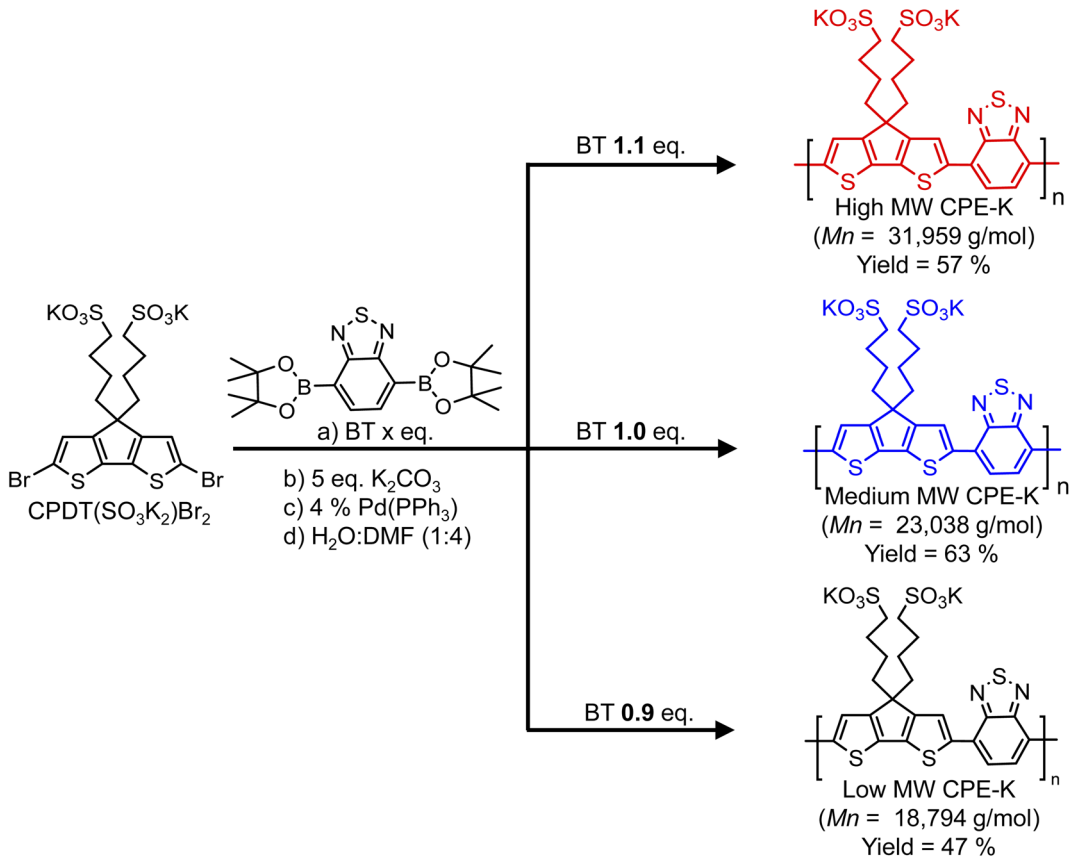

Fig. 2 Synthetic routes for obtaining high, medium, and low MW CPE-Ks with their respective yields. Equivalents were determined by the weight of the reactants used; see ESI† for complete details.

electrolyte reservoir, see Fig. S7.†[14] The potential window was constrained from −0.5 V to 0.6 V (all electrochemical measurements are reported *vs.* Ag/AgCl saturated KCl) to avoid irreversible electrochemical reactions in the aqueous electrolyte solution and Au oxidation, which happens at potentials >0.6 V.[26] As shown in Fig. 3A, one observes CV curves with quasi-rectangular shapes, indicative of pseudocapacitive characteristics.[4,20,27] Furthermore, the CV traces are symmetric along the *x*-axis with a coulombic efficiency of ~100%, calculated from the ratio of charges (Q) involved in the discharge process to that of the charging process, see Fig. S8.† The initial coulombic efficiency was 97% for the high MW CPE-K hydrogel, while it was 93% and 90% for the medium and low MW CPE-K counterparts, respectively, indicating that increasing MW results in higher electrochemical reversibility.[28,29] Moreover, increasing the MW of CPE-K also decreases the onset oxidation potential for the pseudocapacitive process. Specifically, the high MW CPE-K hydrogel exhibits an oxidation peak potential of ~0.17 V, which is significantly lower than those observed in the medium and low MW CPE-K hydrogels (0.33 V and 0.41 V, respectively). A lower onset potential translates to a wider pseudocapacitive potential window, a desirable feature for achieving higher capacitance.[3]

Galvanostatic charge/discharge (GCD) measurements were performed to determine the capacitance of CPE-K gels through the use of eqn (1):

$$C = I \times \Delta t/m \times \Delta V \quad (1)$$

where I is the constant discharge current, Δt is the discharge time, m is the mass of the CPE-K, and ΔV is the discharging voltage drop (excluding *IR* drop). The potential window was set between 0.2–0.6 V.[20] These studies show that increasing the MW of CPE-K consistently boosts the specific capacitance at each specific current tested, see Fig. 3B and Table S1.† For instance, at $\langle J \rangle = 0.25$ A g^{-1}, the high MW CPE-K exhibits a specific capacitance of 88 ± 4 F g^{-1}, which is higher relative to that obtained for the medium (78 ± 8 F g^{-1}) and low (71 ± 9 F g^{-1}) MW CPE-K. From the measured capacitance values, we can estimate the doping level of the CPE-K gel network based on the following eqn (2):

$$C = \alpha \times F/\Delta E \times M \quad (2)$$

where α is the doping level per monomer unit, F is the Faraday constant (C mol^{-1}), ΔE is the operating voltage range (V), and M is the molecular weight of the monomer (g mol^{-1}).[8]

Quantitative analysis reveals α to be 0.24, 0.22, and 0.20 for the high, medium, and low MW CPE-K, respectively (see Tables 1 and S2†). Taken together, the reduced oxidation onset potential and enhanced doping level in the high MW CPE-K hydrogel indicate a more conductive 3D network. This is further supported by the voltage loss (IR_{drop}) determined from

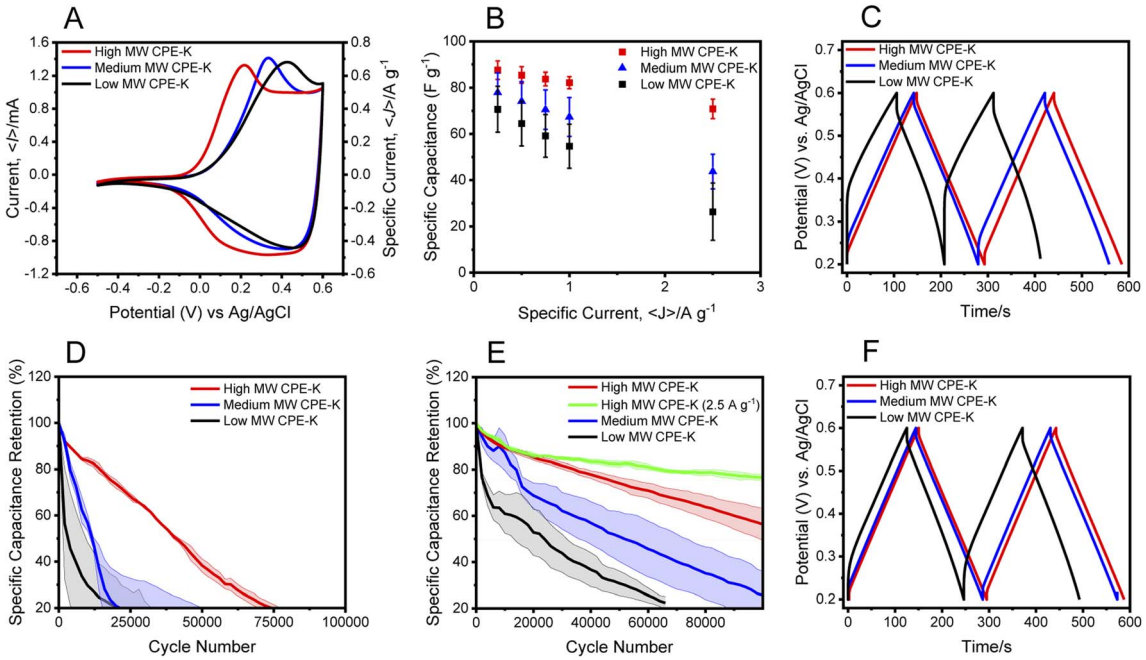

Fig. 3 Representative cyclic voltammetry (CV) as a function of MW (A). Specific capacitance as a function of different specific current values, as calculated by eqn (1) (B). Representative charge/discharge curves of the investigated systems (C) and cycling stability characterization (D) at 1 A g^{-1} in standard medium. Cycling stability characterization (E) at 1 A g^{-1} (unless indicated otherwise) and representative charge/discharge curves of the investigated systems (F) after adding Mg^{2+} into the electrolyte solution. In all cases, measurements were carried out under ambient conditions.

the GCD curves, see Fig. 3C. A systematic reduction in IR_{drop} from 50 mV in the low MW CPE-K to <10 mV in the high MW CPE-K was measured, indicating less internal and diffusion resistance.[30]

Life cycle testing at $\langle J \rangle = 1$ A g^{-1} shows that increasing the MW of CPE-K increases its cycling stability, see Fig. 3D. The high MW CPE-K hydrogel retains ~50% of its original specific capacitance (half-life) value after 41 700 charge/discharge cycles. This performance represents a 3.5-fold improvement compared to its medium MW CPE-K counterpart (after 11 800 charge/discharge cycles) and a 6.4-fold increment compared to its low MW CPE-K counterpart (after 6500 charge/discharge cycles). We further enhanced the cycling stabilities of the hydrogels by adding Mg^{2+} ions (1.6 M) that can serve as interchain crosslinkers.[20] Interestingly, the trend for cycling stability as a function of MW remains the same, see Fig. 3E. Of relevance is that the high MW CPE-K hydrogel retained 56% of its initial specific capacitance after 100 000 cycles at a rate of 1 A g^{-1}. Moreover, 76% of specific capacitance retention after 100 000 cycles was obtained for the high MW CPE-K when measurements were carried out at a rate of 2.5 A g^{-1}, see Fig. 3E. This result is a major advancement since the improvement in stability represents over a 100-fold increment over previously reported CPE-K hydrogels.[11]

We noticed minimal variations in the GCD triangular charge/discharge trace (Fig. 3F) of the high and medium MW CPE-K after adding Mg^{2+}. However, a lengthening in the GCD triangular charge/discharge trace-time and a reduced IR_{drop} (Fig. 3F) were observed for the Low MW CPE-K. Thereby, a significant increase in the pseudocapacitive window (Fig. S9†)

Table 1 Characterization of different hydrogel compositions. The doping percentage (α) was calculated following eqn (1). Kinetic parameters of the CPE-K hydrogels probed by electrochemical impedance spectroscopy (EIS) and cyclic voltammetry (CV); R_{CT} = charge transfer resistance, σ = Warburg factor, b = slope of the log–log plot of $\langle I \rangle$ *vs.* scan rate. G' = gel-like elastic modulus coefficient obtained from rheological measurements. Half-life corresponds to the number of cycles needed for the specific capacitance to arrive at 50% of its original value

System	α	b (≤60 mV s^{-1})	R_{CT} (Ω)	σ (Ω $s^{-1/2}$)	G' (Pa)	Half-life (cycle number)
High MW CPE-K	0.24	0.84	<1	0.95	4173	41 700
Medium MW CPE-K	0.22	0.76	<1	4.64	2520	11 800
Low MW CPE-K	0.20	0.73	<1	5.30	1933	6500
High MW CPE-$K^{Mg^{2+}}$	0.24	0.90	<1	0.43	8273	≥100 000
Medium MW CPE-$K^{Mg^{2+}}$	0.22	0.86	<1	1.50	4320	51 641
Low MW CPE-$K^{Mg^{2+}}$	0.22	0.76	<1	7.17	3208	24 236

and specific capacitance from 73 F g^{-2} to 82 F g^{-2} was obtained (α from 0.20 to 0.22, see Table 1). These observations are in line with our previous results for other low MW CPE-K, as it has been suggested that Mg^{2+} can coordinate a more conductive network by strengthening their inter-molecular interactions.[14,20,31,32]

Quantitative information regarding ionic transport within the hydrogels can be obtained by analyzing the log–log plot of the peak current ($\langle I \rangle$) *vs.* the CV scan rates (Fig. 4A–C) as displayed in Fig. 4D and S10.† This plot obeys the power law in eqn (3):

$$\langle I \rangle \propto \nu^{b} \tag{3}$$

where the slope of the linear fit of the log–log plot is b.[1,33] We noticed that increasing the MW of CPE-K yields a b closer to unity, as b increases from 0.76, to 0.86, and 0.90 for the low, medium, and high MW CPE-K at the scan rate tested ($\leq$60 mV s^{-1}). This trend holds with and without Mg^{2+}, see Fig. S11† and Table 1. These b values indicate a combined surface and diffusion-controlled electrochemical response, consistent with pseudocapacitive behavior, as pseudocapacitors are kinetically limited at low scan rates only by the surface faradaic reactions and at higher scan rates by bulk electrolyte diffusion.[1,33–35] Noteworthy, the surface-controlled regime of the high MW CPE-K hydrogel, as revealed by b, extends to higher scan rates than its lower MW CPE-K counterpart. This behavior indicates superior rate capabilities of the high MW CPE-K hydrogel, as it can maintain efficient ion diffusion kinetics even at high scan rates.[36,37]

Electrochemical impedance spectroscopy (EIS) was used to determine charge transfer resistances and further understand ionic mobility. The data were fitted to an equivalent circuit that included an additional circuit element in series called Warburg impedance, W, to accommodate for the ~45° linear response at low frequencies. This gave the simplest equivalent circuit RS + (Q_{geom}/R_{CT}) + W, see Fig. S12.†[20,38,39] In all cases, no evident semi-circles were observed from the Nyquist plots of the hydrogels, as shown in Fig. 4E and Table 1, indicating minimal charge transfer resistance ($R_{CT} \leq 1$ ohm). That the Nyquist plot for the high MW CPE-K becomes more vertical at lower frequencies indicates more facile ion diffusion.[40] Warburg resistance contributions can be obtained by analyzing the response of Z' *versus* the inverse of the square root of the frequency ($\omega^{-1/2}$), as shown in eqn (4):

$$Z' = R_E + R_{CT} + \sigma\omega^{-1/2} \tag{4}$$

where R_E is the resistance between the electrolyte and the electrode, R_{CT} is the charge transfer resistance, ω is the angular frequency, and σ is the Warburg factor.[41] Based on this relationship, the slope of the linearly fitted lines of Z' *vs.* $\omega^{-1/2}$ provides σ. This analysis reveals that increasing the MW of CPE-K results in a smaller σ, see Fig. 4F and S13.† Specifically, the σ value of the high MW CPE-K hydrogel (0.38 Ω $s^{-0.5}$) is 4.2 times smaller than that of the medium MW CPE-K (1.6 Ω $s^{-0.5}$) and 9.2 times smaller than that of the low MW CPE-K (3.5 Ω $s^{-0.5}$), indicating that the electrochemical behavior of the hydrogel composed of the high MW CPE-K benefits from faster ionic

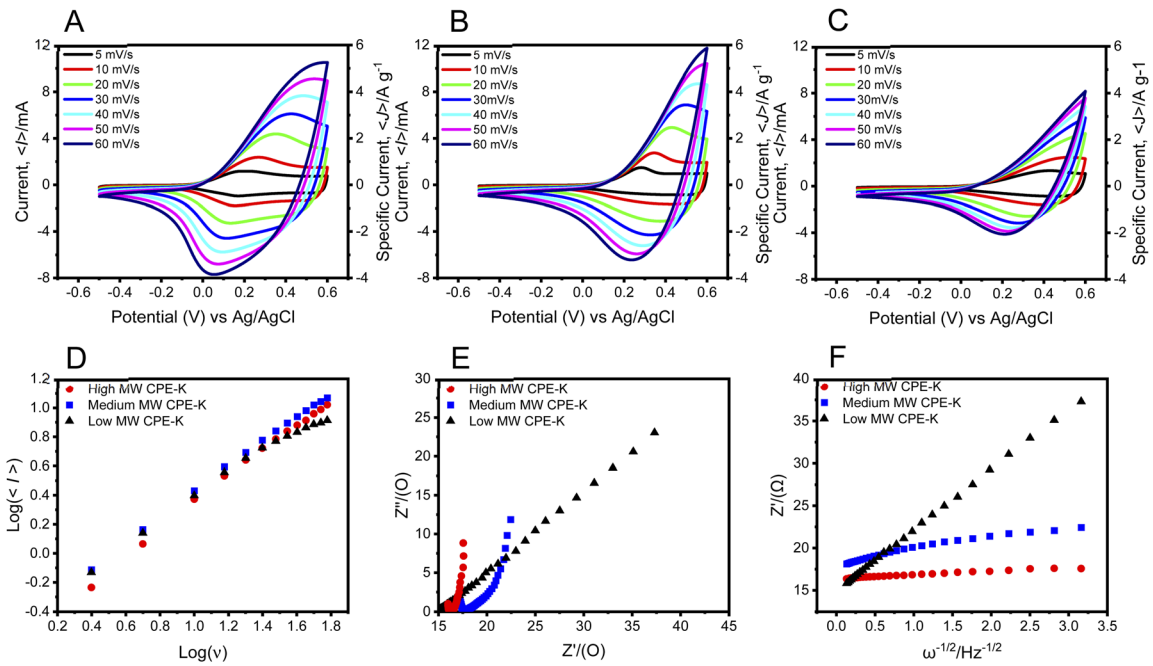

Fig. 4 Scan-rate dependent CV traces of the high (A), medium (B), and low (C) MW CPE-K hydrogels after stabilization. Log–log plot of peak current *vs.* scan rate comparison among the investigated CPE-Ks (D). Nyquist-plot comparison of the high, medium, and low MW CPE-K hydrogels after stabilization (E) and the relationship of Z' and $\omega^{-1/2}$ of the investigated systems for determining the Warburg factor (F), both obtained *via* electrochemical impedance spectroscopy (EIS). In all cases, measurements were carried out under ambient conditions after adding Mg^{2+} into the supporting electrolyte.

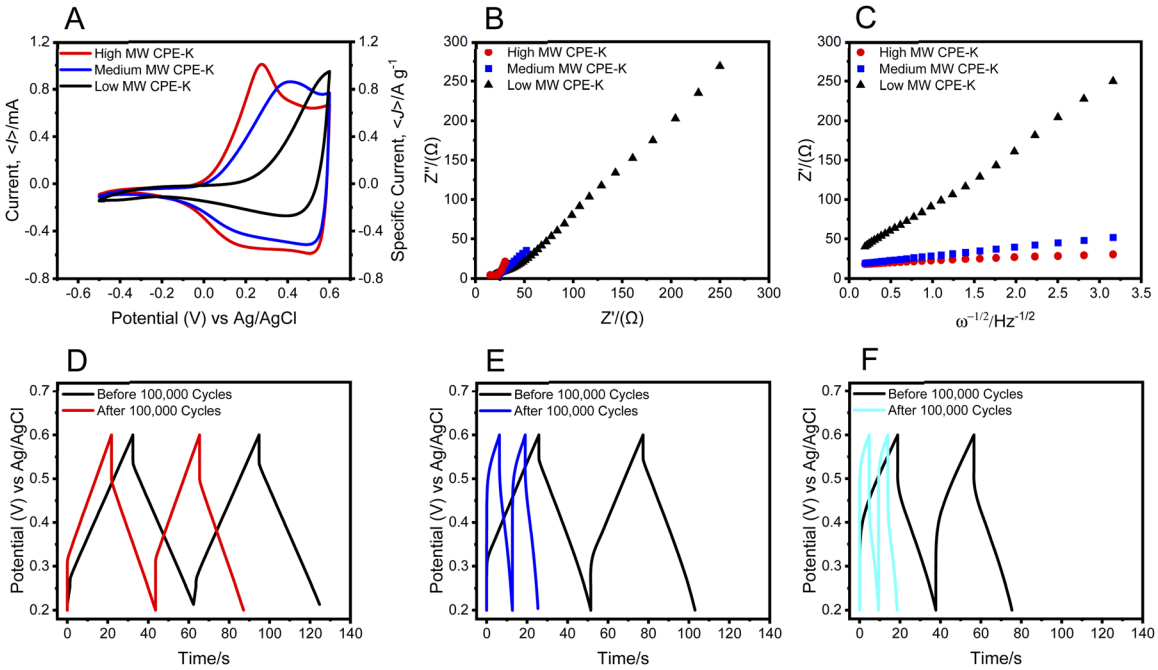

Fig. 5 Representative CV (A), Nyquist (B), and Z' *vs.* $\omega^{-1/2}$ (C) plots of the investigated hydrogels before and after life cycle testing. GCD traces for the high (D), medium (E), and low (F) MW CPE-K before and after life cycle testing. All measurements were carried out under ambient conditions after adding Mg^{2+} into the electrolyte solution.

diffusion kinetics.[11,40] This trend holds with and without Mg^{2+} (Fig. S14†) and is in line with the analysis above of the log–log plots of $\langle I \rangle$ *vs.* scan rates, which show higher rate capabilities of the high MW CPE-K hydrogel, see Table 1.[33] Initially, these results were counterintuitive, based on our original thinking that the high MW CPE-K would provide a more viscous medium for ion transport. However, these findings reveal that increasing the MW of CPE-K results in hydrogels with less internal and ionic resistances.[11,20] Our current thinking is that the higher MW of CPE-K provides a higher degree of percolation for ion migration and electronic communication within the 3D conductive network. As a result, the redox-active sites of CPE-K are more accessible to anions for ionic–electronic coupling during charging, explaining the α enhancement.[20,42]

Next, we investigate the mechanism of specific capacitance loss by evaluating the electrochemical response of the CPE-Ks after life cycle testing, see Fig. 5. As observed in Fig. 5A, all CPE-Ks show a narrowing in their pseudocapacitive potential window in parallel with increments in their ionic resistances, see Fig. 5B. Specifically, the σ values for the high, medium, and low MW CPE-K were 7.9 $\Omega\ s^{-1/2}$, 11 $\Omega\ s^{-1/2}$, and 51 $\Omega\ s^{-1/2}$, which are at least five times higher than their initial values, see Fig. 5C, S15† and Table 2. In all cases, the IR_{drop} values obtained from GCD also increased, see Fig. 5D–F. That the high MW CPE-K still possesses the highest pseudocapacitive window, ionic conductivity, and lowest IR_{drop} indicates that increasing the MW of CPE-K helps to better preserve the structural integrity of the conductive network during multiple charge/discharge cycles. Optical absorption spectra of CPE-K before and after GCD characterization (Fig. S16†) reveals no noticeable wavelength shifts of the peaks and no changes to the relative contributions of neutral and polaronic states, implying no chemical degradation of CPE-K. Therefore, the observed decay in capacitance is attributed predominantly to structural changes of the hydrogel.

We rely on rheological measurements to understand the mechanical properties of the investigated gels.[16] As shown in Fig. 6A and S17,† all obtained G' and G'' values are independent of frequency and $G' > G''$ across the measured frequency range, indicating that all systems indeed exhibit hydrogel-like characteristics.[16,43] The positive correlation between MW of CPE-K

Table 2 Electrochemical characterization summary before and after cycling stability measurements was carried out. σ = Warburg factor. The anodic shifts are the differences between the oxidation peak maxima before and after GCD characterization. Measurements were conducted under ambient atmosphere with Mg^{2+} added to the electrolyte solution

System	σ ($\Omega\ s^{-1/2}$) before GCD	σ ($\Omega\ s^{-1/2}$) after GCD	Potential maxima (V) before GCD	Potential peak maxima (V) after GCD	Anodic shift (V)
High MW CPE-K	0.43	7.9	0.17	0.27	0.10
Medium MW CPE-K	1.5	11	0.33	0.43	0.10
Low MW CPE-K	7.2	51	0.41	0.6	0.19

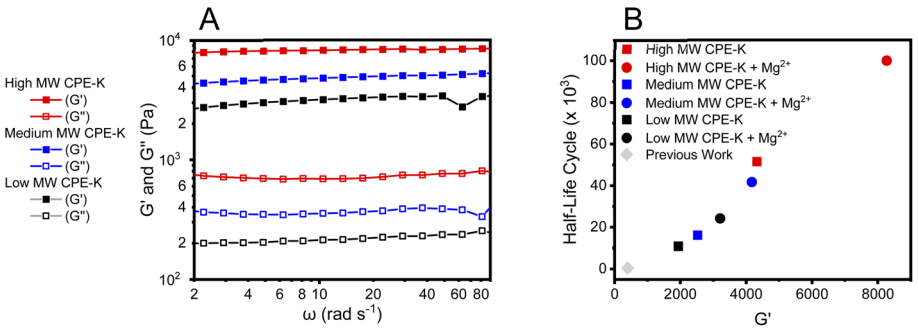

Fig. 6 Rheological measurements of the investigated systems after adding Mg^{2+} into the electrolyte solution (A). Half-life cycling stability of the CPE-K hydrogels *vs.* their respective G' value before and after adding Mg^{2+} into the electrolyte solution (B). One can notice the correlation between the G' and the half-life cycling of the hydrogel. All measurements were carried out under ambient conditions.

and G' indicates that increasing the MW of CPE-K results in hydrogels with greater mechanical strength. In the case with Mg^{2+} added (Fig. 6A), the high MW CPE-K possesses a G' (8273 Pa) 1.9 larger than that of the medium MW CPE-K (4.320 Pa) and 2.6 times larger than that of the low MW CPE-K (3208 Pa). We note that the higher mechanical strength of the CPE-K hydrogel is correlated to better cycling stability (Fig. 6B), lower internal and solution resistances, and higher specific capacitance. These results are in line with our general thinking that longer chains in the high MW CPE-K give rise to stronger inter-chain contacts for more robust morphological organization and entangled chains with a higher degree of percolation within the 3D conductive network.[44] As a result, improved cycling stability of the high MW CPE-K is obtained due to higher tolerance to structural degradation associated with volumetric changes upon multiple charge/discharge cycles.

3 Conclusion

This study shows that increasing the MW of CPEs used in pseudocapacitive hydrogels is an effective strategy for enhancing specific capacitance, electrical/ionic percolation, mechanical stability, and cycling stability. Using CPE-K hydrogel as a model system, the high MW CPE-K employed in this work exhibits a specific capacitance of 88 ± 4 F g^{-1} and a remarkable cycling stability of 76% capacitance retention after 100 000 cycles. Rheological measurements correlated more robust hydrogels with an enhanced electrochemical response. Our current thinking is that the higher MW promotes stronger inter-chain contacts, resulting in entangled polymeric chains with well-defined ionic channels within the 3D conductive network of the hydrogel. As a result, (1) the redox-active sites of CPE-K are more accessible for ionic–electronic coupling during charging, explaining the α enhancement, and (2) the hydrogel is more tolerant to volumetric changes upon multiple cycles. These findings provide a new strategy to optimize the physico-electrochemical properties of CPE-based hydrogels and are complementary to conventional approaches of employing interchain cross-linking additives.

Author contributions

Vázquez, Quek, and Bazan conceptualized the idea, designed the experiments, and co-wrote the manuscript. Vázquez and Quek synthesized and structurally characterized the compounds while Llanes ran and analyzed the GPC measurements. McCuskey and Wang contributed with in-depth CV and EIS analysis pertinent to ion conductivity. Kundukad did the rheological measurements. Vázquez and Quek contributed equally to this work.

Conflicts of interest

The authors declare no conflict of interest.

Acknowledgements

This research was supported by the Ministry of Education, Singapore, under its Research Centre of Excellence award to the Institute for Functional Intelligent Materials (I-FIM, project No. EDUNC-33-18-279-V12) and by the National University of Singapore start-up grant A-0004525-00-00. Work at SCELSE was supported by core research funds, SCELSE is funded by the National Research Foundation, Ministry of Education, Nanyang Technological University (NTU), and National University of Singapore (NUS) and hosted by NTU in partnership with NUS.

References

1 J. C. Russell, V. A. Posey, J. Gray, R. May, D. A. Reed, H. Zhang, L. E. Marbella, M. L. Steigerwald, Y. Yang, X. Roy, C. Nuckolls and S. R. Peurifoy, *Nat. Mater.*, 2021, **20**, 1136–1141.
2 X. Yu, S. Yun, J. S. Yeon, P. Bhattacharya, L. Wang, S. W. Lee, X. Hu and H. S. Park, *Adv. Energy Mater.*, 2018, **8**, 1–33.
3 C. Choi, D. S. Ashby, D. M. Butts, R. H. DeBlock, Q. Wei, J. Lau and B. Dunn, *Nat. Rev. Mater.*, 2020, **5**, 5–19.
4 S. Fleischmann, J. B. Mitchell, R. Wang, C. Zhan, D. Jiang, V. Presser and V. Augustyn, *Chem. Rev.*, 2020, **120**, 6738–6782.

5 K. C. S. Lakshmi, X. Ji, T.-Y. Chen, B. Vedhanarayanan and T.-W. Lin, *J. Power Sources*, 2021, **511**, 230434.
6 J. F. Ponder, A. M. Österholm and J. R. Reynolds, *Chem. Mater.*, 2017, **29**, 4385–4392.
7 T. Liu, L. Finn, M. Yu, H. Wang, T. Zhai, X. Lu, Y. Tong and Y. Li, *Nano Lett.*, 2014, **14**, 2522–2527.
8 K. D. Fong, T. Wang and S. K. Smoukov, *Sustainable Energy Fuels*, 2017, **1**, 1857–1874.
9 K. D. Fong, T. Wang, H.-K. Kim, R. V. Kumar and S. K. Smoukov, *ACS Energy Lett.*, 2017, **2**, 2014–2020.
10 Z. Yang, D. Shi, W. Dong and M. Chen, *Chem.–Eur. J.*, 2020, **26**, 1846–1855.
11 G. Quek, B. Roehrich, Y. Su, L. Sepunaru and G. C. Bazan, *Adv. Mater.*, 2022, **34**, 2104206.
12 M. D. Ingram, H. Staesche and K. S. Ryder, *J. Power Sources*, 2004, **129**, 107–112.
13 G. Quek, R. J. Vázquez, S. R. McCuskey, B. Kundukad and G. C. Bazan, *Adv. Mater.*, 2022, 2203480.
14 G. Quek, Y. Su, R. K. Donato, R. J. Vázquez, V. S. Marangoni, P. R. Ng, M. C. F. Costa, B. Kundukad, K. S. Novoselov, A. H. C. Neto and G. C. Bazan, *Adv. Electron. Mater.*, 2022, **8**, 2100942.
15 T. Sheng, X. Guan, C. Liu and Y. Su, *ACS Appl. Mater. Interfaces*, 2021, **13**, 52234–52249.
16 S. P. O. Danielsen, G. E. Sanoja, S. R. McCuskey, B. Hammouda, G. C. Bazan, G. H. Fredrickson and R. A. Segalman, *Chem. Mater.*, 2018, **30**, 1417–1426.
17 S. R. McCuskey, Y. Su, D. Leifert, A. S. Moreland and G. C. Bazan, *Adv. Mater.*, 2020, **32**, 1908178.
18 K. Wang, X. Zhang, C. Li, H. Zhang, X. Sun, N. Xu and Y. Ma, *J. Mater. Chem. A*, 2014, **2**, 19726–19732.
19 R. J. Vázquez, S. R. McCuskey, G. Quek, Y. Su, L. Llanes, J. Hinks and G. C. Bazan, *Macromol. Rapid Commun.*, 2022, 2100840.
20 Y. Su, S. R. McCuskey, D. Leifert, A. S. Moreland, L. Zhou, L. C. Llanes, R. J. Vazquez, L. Sepunaru and G. C. Bazan, *Adv. Funct. Mater.*, 2021, **31**, 2007351.
21 D. Yang, *Chem. Mater.*, 2022, **34**, 1987–1989.
22 C. Hu, Y. Lin, J. W. Connell, H. M. Cheng, Y. Gogotsi, M. M. Titirici and L. Dai, *Adv. Mater.*, 2019, **31**, 1–14.
23 P. Simon and Y. Gogotsi, *Materials for Sustainable Energy*, 2010, **7**, 138–147.
24 R. Iwamori, R. Sato, J. Kuwabara and T. Kanbara, *Polym. Chem.*, 2022, **13**, 379–382.
25 P. A. Cox, A. G. Leach, A. D. Campbell and G. C. Lloyd-Jones, *J. Am. Chem. Soc.*, 2016, **138**, 9145–9157.
26 O. Diaz-Morales, F. Calle-Vallejo, C. De Munck and M. T. M. Koper, *Chem. Sci.*, 2013, **4**, 2334–2343.
27 T. S. Mathis, N. Kurra, X. Wang, D. Pinto, P. Simon and Y. Gogotsi, *Adv. Energy Mater.*, 2019, **9**, 1902007.
28 Q. Wei, Q. Li, Y. Jiang, Y. Zhao, S. Tan, J. Dong, L. Mai and D.-L. Peng, *Nano-Micro Lett.*, 2021, **13**, 55.
29 G. Choi, J. Kim and B. Kang, *Chem. Mater.*, 2019, **31**, 6097–6104.
30 H. Gul, A.-H. A. Shah, U. Krewer and S. Bilal, *Nanomaterials*, 2020, **10**, 118.
31 F. Wurm, B. Rietzler, T. Pham and T. Bechtold, *Molecules*, 2020, **25**, 1840.
32 K. Zhang, Q. Feng, J. Xu, X. Xu, F. Tian, K. W. K. Yeung and L. Bian, *Adv. Funct. Mater.*, 2017, **27**, 1–11.
33 V. Augustyn, J. Come, M. A. Lowe, J. W. Kim, P.-L. Taberna, S. H. Tolbert, H. D. Abruña, P. Simon and B. Dunn, *Nat. Mater.*, 2013, **12**, 518–522.
34 B. E. Conway, *Proc. Int. Power Sources Symp.*, 1991, 319–327.
35 V. Augustyn, P. Simon and B. Dunn, *Energy Environ. Sci.*, 2014, **7**, 1597.
36 Y. Huang, M. Zhong, Y. Huang, M. Zhu, Z. Pei, Z. Wang, Q. Xue, X. Xie and C. Zhi, *Nat. Commun.*, 2015, **6**, 10310.
37 S. K. Meher and G. R. Rao, *J. Phys. Chem. C*, 2011, **115**, 25543–25556.
38 H. Li, J. Wang, Q. Chu, Z. Wang, F. Zhang and S. Wang, *J. Power Sources*, 2009, **190**, 578–586.
39 J. Wang, S. Dong, B. Ding, Y. Wang, X. Hao, H. Dou, Y. Xia and X. Zhang, *Natl. Sci. Rev.*, 2017, **4**, 71–90.
40 X. Wang, S.-M. Bak, M. Han, C. E. Shuck, C. McHugh, K. Li, J. Li, J. Tang and Y. Gogotsi, *ACS Energy Lett.*, 2022, **7**, 30–35.
41 W. Liu, H. Yi, Q. Zheng, X. Li and H. Zhang, *J. Mater. Chem. A*, 2017, **5**, 10928–10935.
42 F. Béguin, V. Presser, A. Balducci and E. Frackowiak, *Adv. Mater.*, 2014, **26**, 2219–2251.
43 B. Kundukad, T. Seviour, Y. Liang, S. A. Rice, S. Kjelleberg and P. S. Doyle, *Soft Matter*, 2016, **12**, 5718–5726.
44 A. Han and R. H. Colby, *Macromolecules*, 2021, **54**, 1375–1387.